JOURNAL OF SOLID STATE CHEMISTRY 112, 376–380 (1994)

Infrared Spectra and Seebeck Coefficient of $LnCoO_3$ with the Perovskite Structure

Yoo Young Kim

Department of Chemistry, Jeonju University, Jeonju 560-759, Korea

Dong Hoon Lee

Department of Chemistry, Yonsei University, Seoul 120-749, Korea

and

Tae Yun Kwon and Sung Ho Park

Department of Chemistry, Jeonju University, Jeonju 560-759, Korea

Received August 19, 1993; in revised form November 23, 1993; accepted November 29, 1993

The lattice vibrations in $LnCoO_3$ perovskites (Ln = La, Pr, Nd, Sm, Eu, or Gd) have been investigated with reference to the lattice vibrations of the ideal cubic perovskite. These vibrations at room temperature indicate the structural changes with the change in the Ln ion. These frequencies are helpful in estimating the stability of the synthesized $LnCoO_3$ phase. The temperature dependence of vibrational frequencies and the Seebeck coefficient reveal that the crystal symmetry is unchanged and the spin transition is due to the entropy increase of the 3*d* electrons with rising temperature.

INTRODUCTION

Oxides with the formula ABO_3 in which A and B cations are coordinated by 12 and 6 oxygen ions, respectively, have the perovskite structure. The B-site ions and B–O bonds play a crucial role in determining the properties of these oxides. We are particularly interested in compounds with the formula $LnCoO_3$ (Ln = La or rare earth element), because they exhibit the spin transition, localized ↔ collective electrons, of the 3*d* electrons in the trivalent Co ion in temperature variations (1–4). This transition temperature increases with the decreasing radius of the Ln ion (3–5).

Infrared spectrometry of oxides is a good technique for determining structures and bonding characteristics. The general form of the lattice vibrations is determined by the use of lattice-symmetry arguments. The lattice vibrations in the structures of low symmetry in the perovskite structure can be approximately inferred from these of the ideal cubic perovskite (6). The complexity of lattice vibrations results from the decrease in the degree of degeneracy in the structures of low symmetry. The decrease in the degree of degeneracy increases the number of the infrared-active lattice vibrations (6, 7), and the number of the observed absorption bands in the spectrum of the material with the low symmetry is expected to increase correspondingly. However, in the case of $BaTiO_3$, which exhibits phase transitions with temperature variations, the absorption bands are clearly separated in the spectrum of the rhombohedral rather than of the orthorhombic or tetragonal symmetries (6). In general, the vibrational energy is proportional to the square root of the bond strength and inversely proportional to the square root of the atomic mass. In the lattice vibrations of $BaTiO_3$, because the mass effect is invariant with the change in the crystal symmetry, the degree of separation between absorption bands will be determined by the distribution of bond strengths. Therefore, in treating the changes of infrared spectra for compounds of the perovskite structure with the same or similar mass effect it may be reasonable to consider the distribution of bond distances as being related to bond strengths.

On the other hand, the crystal symmetry in $LnCoO_3$ changes from rhombohedral to orthorhombic with the increase of the 4*f* electrons. Accordingly, changes in lattice vibrations with Ln ions in $LnCoO_3$ reveal the changes in the crystal symmetry, the mass effect of the Ln ion, and the bond strengths of the Ln–O and Co–O bonds. The

0022-4596/94 $6.00

changes in absorption bands which include these changes in $LnCoO_3$ are expected to be interpreted in terms of the changes of bond lengths between elements in $LnCoO_3$, compared with those of the ideal cubic perovskite. Here, it may be worth investigating the lattice vibrations for the ideal cubic perovskite. In terms of the normal coordinates, the infrared-active vibrations of the ideal cubic perovskite include the stretching, bending, and external modes. Each mode is triply degenerate (6, 7).

In this study we investigated the effect of using various *Ln* ions in the perovskite structure on the lattice vibrations in $LnCoO_3$; we also studied the changes in spin transition from the temperature dependence of the vibrational frequencies and the Seebeck coefficients.

EXPERIMENTAL

Specimens were prepared by the solid state reaction of binary oxides. Stoichiometric mixtures of CoO and Ln_2O_3 (except that the source of the Pr^{3+} ion was Pr_6O_{11}) were ground and pressed into a disk at 1×10^9 N · m^{-2}. The disk was heated in air for 24 hr on a platinum plate at 1473 K, and then was cooled in air to room temperature.

The structure of the specimen was determined by X-ray powder diffraction using Cu$K\alpha$ radiation with a Philips PW-1710 powder diffractometer and silicon powder as an internal standard. These specimens crystallized in the perovskite structure. $LnCoO_3$, where Ln = Tb^{3+}–Lu^{3+}, could not be synthesized under the above conditions. Lattice parameters were calculated by means of the least squares method.

Infrared spectra, obtained in air at room temperature (8), covered the range 400–900 cm^{-1} using KBr disks with a Shimadzu IR-435 spectrophotometer. The wavenumber was calibrated with a polystyrene film. In order to investigate changes in vibrational frequencies with temperature variations, infrared spectra were measured reversibly between 298 and 510 K for $LaCoO_3$ and $GdCoO_3$.

The Seebeck coefficient from 330 to 1300 K for $LaCoO_3$ and $GdCoO_3$ was determined in a thermal gradient formed horizontally by two independently controled heaters. A mechanical force was applied to both sides of the specimen in order to establish contact between the specimen and Pt plates. The specimen was heated for about 5 hr in the thermal emf specimen holder to 1400 K before being measured. The length of the specimen was greater than 15 mm and the cross section was 1.5×1.5 mm^2. The Seebeck coefficient (Q_T) was obtained from the slope of V vs ΔT at the fixed temperature, where ΔT and V are the temperature difference and potential between both sides of specimen. ΔT, varying from −5 to 5 K, was obtained from the emf difference between double junctions on both sides. The fixed temperature was measured at the position of one of the double junctions, with the polarity of potential taken as positive at the side to which the temperature was measured (Fig. 1). Each potential was measured with a Keithley 192 DMM instrument and the thermocouple used was K-type. The Seebeck coefficients measured with rising and lowering temperatures were consistent. The fact that the signs of Q_T were positive indicates that the charge carriers in $LaCoO_3$ and $GdCoO_3$ are holes.

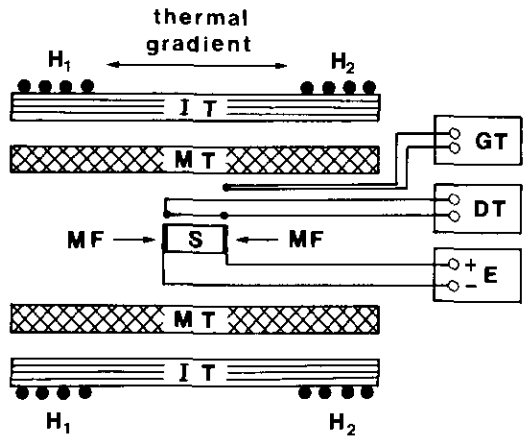

FIG. 1. Schematic for the Seebeck coefficient measurement. S represents the specimen, IT the insulator tube, MT the stainless steel tube, and MF the mechanical force. GT represents the given temperature, and DT is the difference temperature measured as the emf difference in the double junctions. E is the emf of specimen; its polarity is positive at the position GT. H_1 and H_2 are two independently controlled heaters.

RESULTS AND DISCUSSION

I. The Effect of the Ln Ion on Lattice Vibrations

Figure 2 shows that infrared spectra of $LnCoO_3$ consist of two absorption bands associated with the stretching and bending vibrations at 400–900 cm^{-1}. In each spectrum an absorption band at the higher frequency is assigned to the stretching vibration and that at the lower frequency to the bending vibration (6). Absorption bands due to stretching in the $LaCoO_3$ and $PrCoO_3$ spectra are doublets, whereas those due to bending in the $SmCoO_3$, $EuCoO_3$, and $GdCoO_3$ spectra are also doublets; an absorption band due to the bending at the $LaCoO_3$ spectrum is barely observable. The difference between the two frequencies due to the stretching vibration is largest in the $LaCoO_3$ spectrum, whereas an absorption band due to the bending vibration is clearly separated in the $GdCoO_3$ spectrum. Also, other weak absorption bands in the $EuCoO_3$ and $GdCoO_3$ spectra occur below 430 cm^{-1}. These bands are assumed to be due to external vibrations which correspond to the translational motions of *Ln* atoms with respect to CoO_3's in the ideal cubic perovskite. Taking vibrational frequencies into consideration, the change

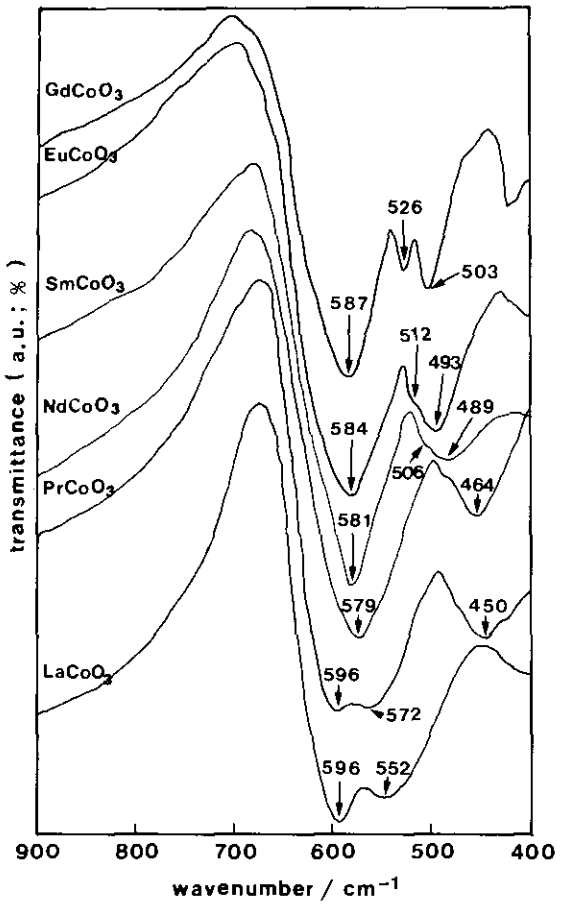

FIG. 2. Infrared spectra of $LnCoO_3$ prepared at 1473 K.

in the bending (ν_b) and external frequencies rather than the stretching frequency (ν_s) with increasing radius of the *Ln* ion is the largest. The changes in absorption bands due to stretching and bending in Fig. 2 do not reflect the changes to the low symmetry configuration. In particular, the changes in the absorption bands are similar to those in infrared spectra of $BaTiO_3$. Therefore, changes in absorption bands in Fig. 2 may be interpreted as arising from the changes in bond distances.

We will first estimate the effect of the trivalent *Ln* ion on the stretching vibration from overlapping bands in the $LaCoO_3$ and $PrCoO_3$ spectra. The trivalent Co ions in $LaCoO_3$, which has two formula units in the rhombohedral cell, are divided into two species, represented by Co_I and by Co_{II}, using the notation defined in Ref. (1). The anion and La^{3+}-ion displacements render the Co_I and Co_{II} ions distinctive, so that the Co_I–O distance is shorter than the Co_{II}–O distance (1). Because the two species produce the same mass effect in the lattice vibrations, the bond strength, i.e., bond distance, dominates the magnitude of the stretching frequency. Therefore, the higher and lower stretching frequencies ($\nu_{s\text{-}h}$ and $\nu_{s\text{-}l}$) correspond to the stretching vibration for Co_I and Co_{II} species, respectively.

Applying these results to the $PrCoO_3$ spectrum, $\nu_{s\text{-}l}$ in the $PrCoO_3$ spectrum is higher by 20 cm^{-1} than in the $LaCoO_3$ spectrum, but the $\nu_{s\text{-}h}$'s are the same. The ionic size of the Pr^{3+} ion may be associated with the increase in $\nu_{s\text{-}l}$ in the $PrCoO_3$ spectrum. As a result of the lanthanide contraction the smaller size of the Pr ion reduces the Pr–O distance; in turn, a decrease in the Co–O distance is expected. The increase in the $\nu_{s\text{-}l}$ and the nearly constant value of $\nu_{s\text{-}h}$ reveal that the decrease in the Pr–O distance shortens the Co_{II}–O distance more readily than the Co_I–O distance. This phenomenon may be associated with the stabilization of each site. Since the crystal field stabilization energy (CFSE) for the cation of the same site and its charge depends on the bond distance, the CFSE for Co_I species will be larger than that for Co_{II}. The fact that the change of the *Ln*–O distance indirectly influences $\nu_{s\text{-}h}$ indicates that the magnitude of CFSE for the dodecahedral field (DFSE), in which the *Ln* ion is located, is lower than that of the octahedral field (OFSE), in which the Co ion is located. This suggests that an increase in DFSE with decreasing Pr–O distance hardly affects the OFSEs for all of cations at the octahedral site in the $PrCoO_3$.

As an electron is added to the 4*f* orbital, the bond distances between elements are reduced. This reduction shows up in the volume per formula unit (V_f). V_f decreases with an increase in the number of 4*f* electrons (Fig. 3). The shrinkage of V_f is correlated with the changes in the observed vibrational frequencies. As the radius of the *Ln* ion is reduced, the *Ln*–O distance approaches a critical

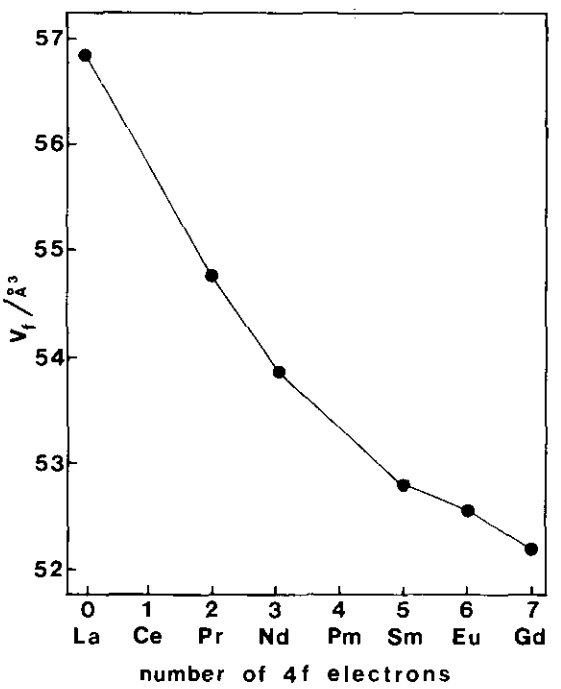

FIG. 3. Plot of the volume per formula unit vs the number of 4*f* electrons.

value at which the Co_I–O and Co_{II}–O distances are equal. If the *Ln*–O distance is shorter than the critical distance, all of Co–O distances must be simultaneously reduced. However, Co–O distances is expected to be slightly decreased from the above result. Accordingly, in order to shrink V_f, *Ln*–O distances are separate into relatively shorter and longer distances, similar to the grouping of Co–O distances in $LnCoO_3$ with the longer *Ln*–O distance than the critical distance. The difference between *Ln*–O distances in two species increases with the decrease of radius of the *Ln* ion. As a result, two species of LnO_{12} dodecahedra induce a zigzagged array of corner-shared CoO_6 octahedra such as encountered in $LnFeO_3$ (9). This phenomenon is reflected in the bending vibration. Two bands due to the bending are clearly found in the $GdCoO_3$ spectrum; $GdCoO_3$ also has the largest degree of zigzag of the CoO_6 octahedra (5). We conclude that changes in Co–O distances are observed in $LnCoO_3$ with the larger *Ln* ion, whereas changes in *Ln*–O distances are revealed in $LnCoO_3$ with the smaller *Ln* ion. Therefore, it is suggested that the ratio of the radius of the *Ln* ion to that of the Co ion determine the crystal symmetry.

From the change in the bending frequencies with changes in the *Ln* ion we can estimate the stability on the synthesized $LnCoO_3$. The higher bending frequencies ($\nu_{b\text{-}h}$) in the $EuCoO_3$ and $GdCoO_3$ spectra are larger by 6 and 20 cm^{-1} than that in the $SmCoO_3$ spectrum. With this trend, the $\nu_{b\text{-}h}$ frequency in $HoCoO_3$ is expected to be about 600 cm^{-1}. This value is equivalent to a stretching frequency. $HoCoO_3$ seems to be the boundary of the stable $LnCoO_3$'s, because the *Ln* ion can be situated at the octahedral site so long as $\nu_b > \nu_h$. However, by the solid state reaction of oxides we could not synthesize $LnCoO_3$ where the number of $4f$ electrons is greater than eight(Tb). The reason appears to be the following: $\nu_{b\text{-}h}$ in $TbCoO_3$ is expected to be about 550 cm^{-1}, which is comparable to the value of the stretching energy in the C-type Tb_2O_3, in which the Tb^{3+} ions are located in distorted octahedral sites (10). This indicates that Tb^{3+} ions in $TbCoO_3$ also tend to be located at octahedral sites. From this result

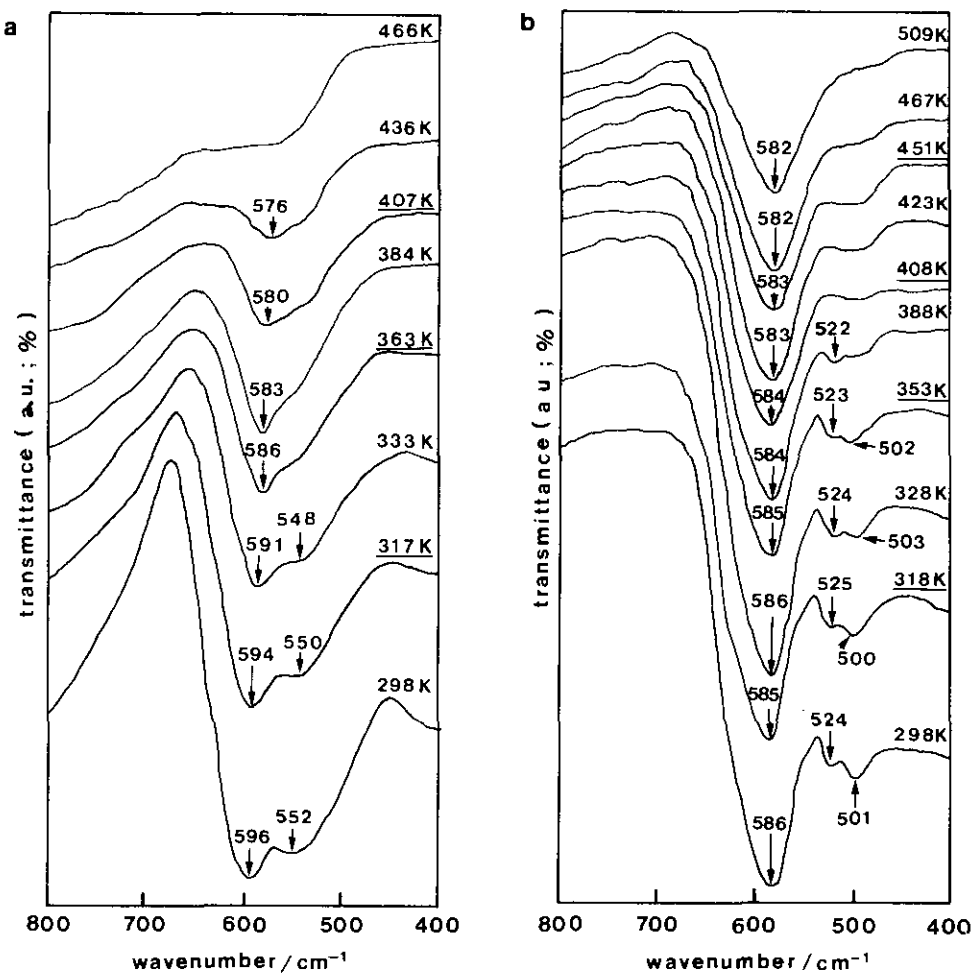

FIG. 4. Infrared spectra measured at various temperatures of 298–510 K for (a) $LaCoO_3$ and (b) $GdCoO_3$. The underlined temperature was measured with decreasing temperatures.

it appears that when ν_b in $LnCoO_3$ is smaller than the vibrational frequency associated with the octahedral *Ln* ion, the corresponding $LnCoO_3$ is unstable. For example, the vibrational frequency ν_b in the stable $YCrO_3$ is 500 cm^{-1} (11). This result is consistent with the fact that the standard Gibbs energy for the reaction ($\frac{1}{2}Ln_2O_3 + CoO + \frac{1}{4}O_2 = LnCoO_3$) is positive between $DyCoO_3$ and $HoCoO_3$ (12); $DyCoO_3$ is stable under an oxygen pressure of 1.3×10^7 Pa (13). In this study, the boundary of the unstable $LnCoO_3$ phase is the Tb ion.

II. Temperature Variations of the Vibrational Frequencies

Infrared spectra measured at various temperatures of 298 to 510 K for $LaCoO_3$ and $GdCoO_3$ in Fig. 4 provide information on spin transitions. Two important considerations in Fig. 4 are the vibrational frequencies and their differences in temperature variations. The higher stretching frequency ($\nu_{s\text{-}h}$) for $LaCoO_3$ is shifted from 595 cm^{-1} at 298 K to 576 cm^{-1} at 436 K, and no band is detected in spectra above 466 K. The differences between two stretching frequencies in three spectra at 298 to 333 K remain constant at 44 cm^{-1}. In Fig. 4b the stretching frequency of 586 cm^{-1} at 298 K is shifted to 582 cm^{-1} at 509 K. The intervals between ν_s and $\nu_{b\text{-}h}$, and between two ν_b's are 62 and 23 cm^{-1}, respectively. Figure 4 shows that, as the temperature is raised, the crystal symmetry of $LnCoO_3$ is not changed.

We relate the change of ν_s in Fig. 4a to the spin transition. In Co_3O_4, which has a low spin $\leftrightarrow$ high spin transition, the temperature dependence of the coefficient of thermal expansion and the Fermi energy (E_F) as determined from the Seebeck coefficient (Q_T) obviously reflect the spin-transition process (14). The E_F is expressed as $E_F = Q_T \cdot e \cdot T$, where e is electron charge and T the absolute temperature. Figure 5 shows the temperature dependence of E_F, which has several inflection points. The decrease of E_F at the maximum reveals the start of the changeover from a low-spin to a high-spin Co matrix. The infrared spectra in Fig. 4a track the transition process. It is not unusual that the generation of the high-spin Co^{3+} ion decreases the vibrational frequencies. On the one hand, since according to Fig. 5 the spin transition of $GdCoO_3$ starts at 540 K, no change in ν_s is expected. In fact, the change in ν_s is 4 cm^{-1}. The fact that the spin transition is a reversible process and starts at the maximum value of E_F suggests that the spin-transition temperature depends on the magnitude of the maximum E_F, and that the spin transition is due to the entropy increase of the six $3d$ electrons in the t_{2g} band as the temperature is raised. Therefore, additional studies for materials in which the Co ions are located at the octahedral sites are necessary.

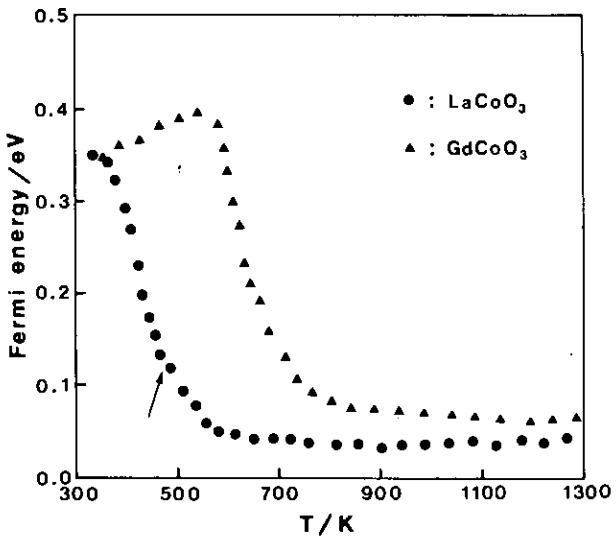

FIG. 5. Plot of Fermi energy vs the absolute temperature. The Fermi energy is calculated from $E_F = Q_T \cdot e \cdot T$, using the Seebeck coefficient. The arrow indicates the temperature of an infrared spectrum in which an absorption band due to the stretching vibration cannot be detected.

ACKNOWLEDGMENT

The authors are grateful to Dr. E. J. Oh, Department of Chemistry, Myungji University, for help in measuring the Seebeck coefficient.

REFERENCES

1. P. M. Raccah and J. B. Goodenough, *Phys. Rev.* **155,** 932 (1967).
2. V. G. Bhide, D. S. Rajoria, Y. S. Reddy, G. R. Rao, and C. N. R. Rao, *Phys. Rev. B* **8,** 5028 (1973).
3. W. H. Madhusudan, K. Jagannathan, P. Gangul, and C. N. R. Rao, *J. Chem. Soc. Dalton* 1397 (1980).
4. G. Thornton, F. C. Morrison, S. Partington, B. C. Tofiel, and D. E. Williams, *J. Phys. C* **21,** 2871 (1988).
5. X. Liu and C. T. Prewitt, *J. Phys. Chem. Solids* **52,** 441 (1991).
6. J. T. Last, *Phys. Rev.* **105,** 1740 (1957).
7. S. Tajima, A. Masaki, S. Uchida, T. Matsuura, K. Fueki, and S. Sugai, *J. Phys. C* **20,** 3469 (1987).
8. Y. Y. Kim, K. H. Kim, and J. S. Choi, *J. Phys. Chem. Solids* **50,** 903 (1989).
9. S. Geller, *J. Chem. Phys.* **24,** 1236 (1956).
10. M. W. Urban and B. C. Corlinsen, *J. Phys. Chem. Solids* **48,** 475 (1987).
11. P. S. Patil, N. Venkatramni, and V. K. Rohatgi, *J. Mater. Sci. Lett.* **7,** 413 (1988).
12. K. Katayama, *J. Solid State Chem.* **76,** 241 (1988).
13. J. P. Coutures, J. M. Badie, R. Berjoan, J. Coutures, R. Flamand, and A. Rouanet, *High Temp. Sci.* **13,** 331 (1980).
14. A. D. D. Broemme, *IEEE Trans. Electr. Insul.* **26,** 49 (1991).